Magnetic field continuity conditions in finite element analysis

Y. Lefevre, C. Henaux and J.F. Llibre
LAPLACE, University of Toulouse - CNRS, Toulouse, 31071 FRANCE, {lefevre, henaux, llibre}@laplace.univ-tlse.fr

This paper deals with the magnetic field continuity conditions in finite element analysis. Our study is based on numerical and analytical models. Different known finite element codes, based on 2D nodal finite element or 3D edge element, are used to analyze the magnetic field in a linear motor like device. The use of an analytical model gives interesting insight on interface errors problems in finite element analysis.

***Index Terms*— Analytical model, Finite element analysis, Magnetic devices, Magnetic fields.**

I. INTRODUCTION

THE normal component B_n of the magnetic flux density $\boldsymbol{B}$ and the tangential component H_t of the magnetic field intensity $\boldsymbol{H}$ satisfy the field continuity conditions at the interface of two media of different permeability values. It has been known that in FEM there are interface error problems due to the fact that only one continuity condition is imposed strongly by FEM [1][2]. This paper analyses in a simple device these interface error problems. As most of applications required only a 2D numerical calculation, we will use first 2D nodal finite element method. In some applications, as in axial flux motor, 3D numerical calculation is needed. 3D edge finite element method will be used. Edge elements have been developed to overcome some drawbacks of 3D nodal finite element [3]. First the studied device is presented. Then the study of the interface error problems on our simple device is performed with different numerical models. Eventually, analytical model is used to theoretically analyze the results obtained.

II. STUDIED SLOTLESS DEVICE AND FEM COMPUTATIONS

In order to quantify interface errors, the distribution of magnetic field inside a permanent magnet linear motor like device is analyzed by two different FEM based software: 2D nodal finite element and 3D edge element. The geometry of the motor is very simple. Fig. 1 shows a pole pitch of this device. It is easy to see where the permanent magnet and airgap are. Above the airgap is the upper plate made of iron and under the permanent magnet is the bottom plate made also of iron. Above the upper plate and under the bottom plates there is air. The permanent magnet is polarized in the vertical axis O_y. Axis O_x is horizontal. A slotless motor like is chosen in order to avoid corner effects that may affect the analyses.

A. *Mesh used for 2D nodal FEM and 3D edge FEM*

Different meshes of the domain have been obtained. Fig. 1 shows a 2D mesh with a first order triangular element with 14557 elements and 7377 nodes. The mesh in the airgap is very fine. A 3D mesh made of hexahedral edge element will be also used in the final paper.

B. *Distributions of H_t along the interface*

In 2D finite element, generally, a vector potential formulation is used. The continuity of H_t is not imposed. The theory guarantees that if the number of nodes increases the gap between the values of H_t at each side of the interface decreased. As the continuity of B_n is guaranteed, only the continuity of H_t is studied here. The distribution of H_t along the interface has been calculated by different finite element codes with different meshes. Only some results are shown here.

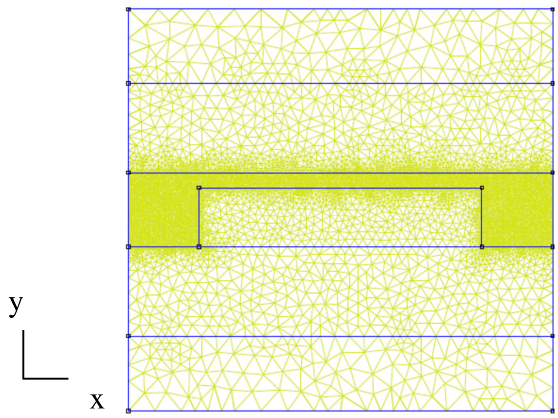

Fig. 1: 2D mesh with first order triangular element.

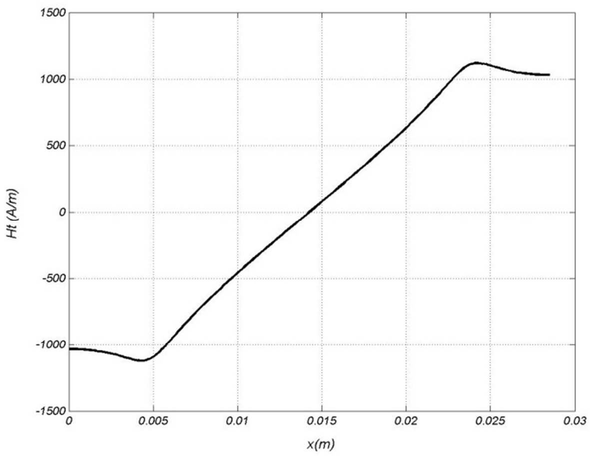

Fig. 2: Distribution of H_t calculated iron side along the interface between airgap and upper plate.

The results obtained using the nodes and elements of the iron side do not change with the type of element, triangular or quadrangular, nor the order of approximation, first order or second order (Fig. 2). For the distribution of H_t calculated from nodes and elements of the airgap, the results change very much with the order of approximation. The distribution obtained from first order element is very different from the distribution calculated in the iron side but it does not change very much with the type of element, triangular or quadrangular (Fig. 3). A huge gap is observed between the two distributions of H_t along the interface (Fig. 2 and Fig. 3).

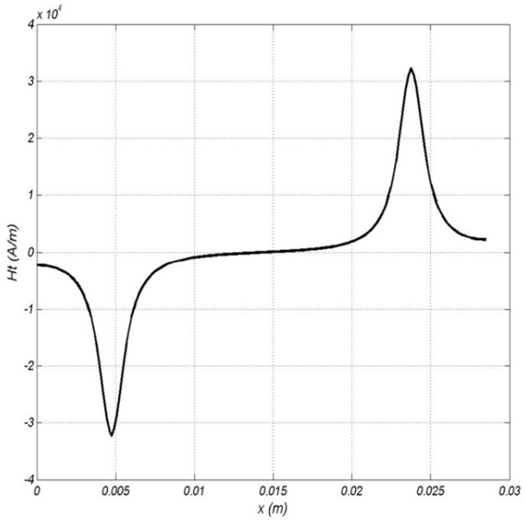

Fig. 3: Distribution of H_t, along the interface, calculated in the airgap side.

The distributions of H_t on the interface has been also calculated by means of a 3D edge element model iron side and airgap side, the results will be shown in the final paper.

III. Analytical model of slotless device

A. Open-circuit magnetic field distribution model

A 2D analytical model of the magnetic field distribution of the studied slotless linear motor can be developed [4]. The continuity conditions have been taken into account. In this model, both continuity conditions are strongly imposed.

B. Distributions of Ht along line parallel to Ox

The distributions of H_t along lines parallel to the horizontal axis O_x have been calculated along four lines in the airgap and in the 'upper plate' iron. The first of these lines L_1 is, in each case, the interface between airgap and 'upper plate'. The distributions along these lines are shown on Fig. 4 and Fig. 5. These results show first that the variation of H_t in function of the distance to the interface is very strong almost exponentially in the airgap. This variation is hardly described by FEM unless a very fine mesh is used. It can explain why the computation of electromagnetic force and torque regularly leads to uncertain results that are strongly dependent on the applied mesh [5]. These results shown on Fig. 2, Fig. 4 and Fig. 5 also that the analytical model and the FEM model give the same distribution along the interface calculated iron side (curve L_1 on Fig. 4 and Fig. 5).

IV. Conclusion

Theoretical considerations on FEM lead to the conclusions that interface errors are inherent to the weak formulation used in FEM. Gaps of H_t on interface are observed with 2D nodal FEM. An analytical model of the magnetic field shows that the variation of H_t with the distance from the iron-airgap interface is so strong that first order finite element may hardly succeed to account of it. Results obtained from second order 2D fem and 3D edge element will be analysed in the final paper.

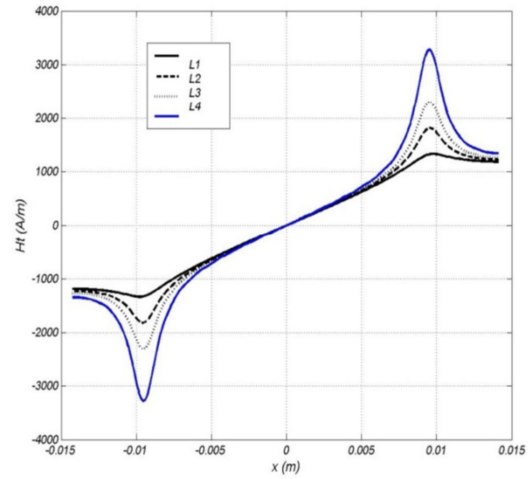

Fig. 4: Distributions of H_t along lines L_1, L_2, L_3 and L_4 in the airgap.

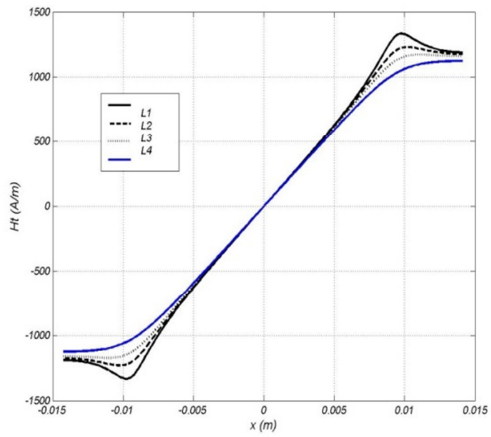

Fig. 5: Distributions of H_t along lines L_1, L_2, L_3 and L_4 in the iron.

References

[1] A. Bossavit, "How weak is the "weak solution" in finite element methods", IEEE Trans. Magn., Vol. 34, n°5, pp 2429-2432, September 1998.

[2] K. Reichert, R. E. Neubauer, T. Tärnhuvud, "A New Approach Solving the Interface Error Problem of Finite Element Field Calculation Methods by Means of Fictitious Interface Current Sheets or Interface Charges", IEEE Trans. Magn., Vol. 28, n°2, pp 1696-1699, March 1992

[3] J. Jin,"The finite element method in electromagnetics", 2nd Edition, Wiley-IEEE Press, June 2002.

[4] K. Boughara, B. L. Chikoune, R. Ibtiouen, D. Zarko and O. Touhami, "Analytical Model of Slotted Air-Gap Surface Mounted Permanent-Magnet Synchronous Motor With Magnet Bars Magnetized in the Shifting Direction" *IEEE Trans. on Magnetics*, vol. 45, N° 2, Feb. 2009, pp. 747-758

[5] R. Castillo and J. M. Cañedo, "A 2D Finite-Element Formulation for Unambiguous Torque Calculation" *IEEE Trans. on Magnetics*, vol. 44, N° 3, March 2008, pp. 373—376.